

EXPERIMENTAL AND SCALE UP STUDY OF THE FLAME SPREAD OVER THE PMMA SHEETS

by

**Mojtaba MAMOURIAN, Javad A. ESFAHANI,
and Mohammad B. AYANI**

Original scientific paper

UDC: 662.612.5:66.011

BIBLID: 0354-9836, 13 (2009), 1, 79-88

DOI: 10.2298/TSCI0901079M

To explore the flame spread mechanisms over the solid fuel sheets, downward flame spread over vertical polymethylmethacrylate sheets with thicknesses from 1.75 to 5.75 mm have been examined in the quiescent environment. The dependence of the flame spread rate on the thickness of sheets is obtained by one-dimensional heat transfer model. An equation for the flame spread rate based on the thermal properties and the thickness of the sheet by scale up method is derived from this model. During combustion, temperature within the gas and solid phases is measured by a fine thermocouple. The pyrolysis temperature, the length of the pyrolysis zone, the length of the preheating zone, and the flame temperature are determined from the experimental data. Mathematical analysis has yielded realistic results. This model provides a useful formula to predict the rate of flame spread over any thin solid fuel.

Key words: flame spread, pilot ignition, polymethylmethacrylate, scale up, solid fuel

Introduction

Polymers are used in nearly every commercial buildings, residential house, transportation vehicle, *etc.* Thus the majority of polymer containing end products (cables, carpets, furniture, ...) must pass some type of regulatory test to help assure public safety from fire. To minimize their hazards, the burning behaviors and combustion mechanism should be understood. Polymethylmethacrylate (PMMA) is a transparent material and has excellent corrosion resistance. These advantages make it so popular and widely used in building, industry, and the general consumer products market [1]. Therefore, attention is restricted to PMMA, whose properties are simpler and better understood than those of most other polymeric materials.

Flame spread over the surface of polymeric material is one of the problems in fire researching. Many mathematical and experimental models have been constructed to describe the process of flame spread over a solid fuel. The controlling mechanism of flame spread appears to differ with the surrounding conditions, such as the oxygen concentration [2], or the direction of the gas flow velocity relative to the direction of the flame spread [3, 4]. The flame spread rate depends on the rate of heat transfer from the flame into the preheat region (unburned fuel). The estimation of the heat transfer not only through gas phase but also through solid phase is important for further understanding. Gas phase conductive/convective heat transfer from flame to the solid fuel is the dominate path for downward flame spread [1, 5].

In order to estimate the rate of heat transfer, one needs to know the detail temperature profiles in the gas and solid phases. Esfahani *et al.* [6], and Esfahani [7] determined the history of temperature in the solid and gas phases of the PMMA sample by a numerical model. Fernandes-Pello *et al.* [8, 9], Hirano *et al.* [10], and Krishnamurthy *et al.* [11] measured the histories of surface and interior temperature of PMMA for horizontal flame spread by using of thermocouples.

In the present work, the relation between the flame spread rate and the thicknesses over the thin solid sheets is studied by order of magnitude analysis and investigates the effects of the type of the heat flux on the flame spread rates. The temperature histories were obtained from chart recording of the fine thermocouple output. The lengths of the pyrolysis zone and the preheating zone were extracted from the temperature histories. Analytical results show a good agreement with the experimental results.

Physical model

A sample of thin solid sheet fuel (PMMA) is burned with a slit burner from its top surface and is held in the quiescent environment at a fixed temperature T_∞ . The sample is assumed to be very large in width and length so that, a one-dimensional model is appropriate for spreading behavior. The lengths of the sample are considered without expansion during combustion.

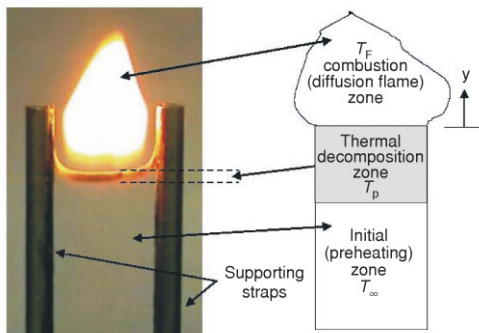


Figure 1. The schematic view of the combustion process in the solid sheet

The solid fuel situated ahead of the flame edge is heated from the ambient temperature to the pyrolysis temperature, T_p . When the temperature of the sample rises, bubbles form and the pyrolysis occurs. The pyrolysis temperature of most polymers is between 180 and 400 °C [4]. When the temperature of the layer exceeds to a pyrolysis temperature, the intensity of gasification is enough to form a diffusion flame. The combustion process occurs as long as the gaseous volatiles are intensively delivered into the reaction zone.

Experimental setup

A schematic of experimental apparatus is shown in fig. 2, according to ASTM 1356. Experiments were carried out under the normal atmospheric conditions, $T_\infty = 300$ K, $P_\infty = 90$ kPa. Sample PMMA sheets are made from various thicknesses of 1.75 to 5.75 mm. The sheets are made by Acrylic Enterprise Co., Ltd. in Taiwan. The dimensions of the sample sheets are 150 mm high and 40 mm wide, set up vertically and ignites at the top edge by a pilot flame. A 25 μ m wire diameter

The schematic of the physical problem is shown in fig. 1. The reaction zone can be divided into three major parts: the initial (preheated zone), thermal decomposition, and combustion zone. In the initial zone, preheating occurs mainly due to absorption of thermal energy and energy transferred through this region by conduction. The thermal decomposition zone, where the rapid thermal decomposition occurs, is due to the convection heat flux from combustion product to the sample. The diffusion flame is formed over this zone which is called combustion zone. For the flame propagation, the most important processes take place in the thermal decomposition zone. The

chromel-alumel thermocouple was used to measure the history of the temperature in solid and gas phases. The thermocouple is pressed into a hole which is drilled in the middle of the sample, about 40 mm under the top edge. At every 1 s, the recorded data by thermocouple is entered to a computer. For each thickness, the test is repeated 3 times to minimize experimental errors.

Experimental results

The temperature distribution for various thicknesses of the sample is shown in fig. 3. It shows that the solid temperature increases gradually (A-B), then it sharply increases (B-C) and reaches to a peak point (C), the pyrolysis temperature about 390 °C, then decreases slightly (C-D) and after (D), it jumps rapidly to a higher level (E). The release volatile of flammable gases moves to the outer atmosphere and mixes with air and absorbed thermal energy. Then the mixture ignites and the temperature in the gas phase increases.

The temperature reaches to a maximum value of about 950 °C (G), and finally falls to the ambient temperature (H). These experimental data is about 7% less than the numerical previous works of Kashani *et al.* [2] and Esfahani *et al.* [6]. This may be, due to the effect of radiation that was neglected in our previous works [2, 6]. The interpretation of the history is the following. The first local maximum pyrolysis region (C) occurs when the junction of the thermocouple moves from the solid into a liquid-like layer adjacent to the surface of the sample. Thereafter, the properties of the sample is changed, and thereby accounting for the temperature to decrease. The first peak (C) and the sudden increase in the recorded temperature (E) provides lower and upper levels for the surface temperature (pyrolysis region) T_{p1} and T_{pu} , respectively. The characteristic length L_p , defined in this level and confirms the result of Fernandez-Pello *et al.* [8]. The observed jump in temperature profile at (E) is due to tension in the junction into the gas phase. The fluctuations of measured temperature are due to variation of gas flow around the thermocouple. The smooth trace in the liquid-like layer (pyrolysis region) seems to indicate that bubbling may not be a problem at high flame spread rates. At lower flame spread rates, due to the difference in the severity of the fluctuations between gas phase and condense phase, thermocouple location is less pronounced. Sometimes observable fluctuations appear prior to the attainment of the first maximum temperature (C). These fluctuations are attributed to bubble formation in the liquid-like layer, a phenomenon which is known to occur at lower flame spread rates. The sharpness of increase of temperature varies from one test to another and may depend on fine details of the manner in which the thermocouple assembly is set into the sample. In some test the jump is difficult to discern, and the levels on the surface temperature are less certain. In these cases the

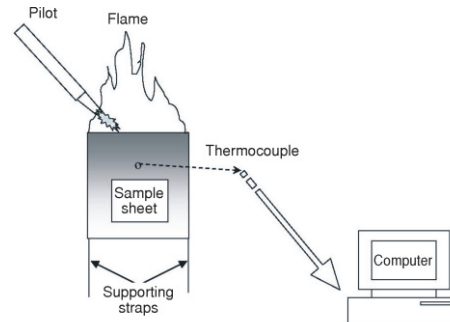


Figure 2. A schematic of the apparatus

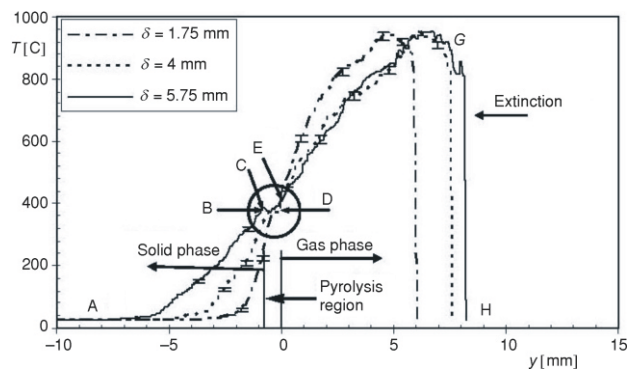


Figure 3. Temperature distribution in the solid and gas phase

first temperature peak is taken as the lower level, and the upper level is placed where gas phase fluctuations clearly become evident.

The temperature distribution in the sample that is shown in fig. 3 indicates that the high temperature zone of solid region is located in the vicinity of the foot of flame. The values of each mode of heat flux shows that the major part of net heat transfer rate into the sample is in this critical zone, and then the energy balance in this zone plays the major role for the flame spread rate [12].

In the thermal decomposition zone, degradation occurred in the characteristic length L_p and it can be obtained at region (C-D) in fig. 3. In the initial zone, preheating occurred in the characteristic length L_s and the temperature increased from initial temperature, T_∞ , to pyrolysis temperature, T_{p1} . Then L_s can be obtained at region (A-B) (for example: if $\delta = 1.75$ mm then, $L_p = 0.2$ mm and $L_s = 2.87$ mm) and it is proportional to thicknesses of the sample and

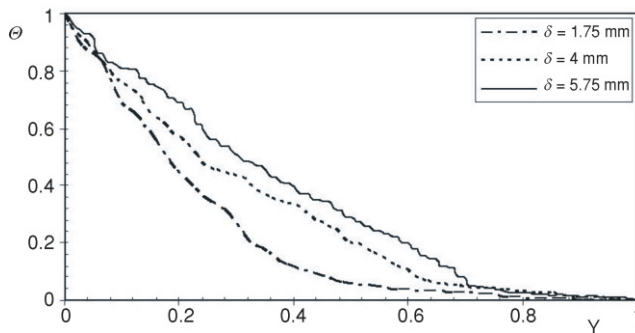


Figure 4. Non-dimensional temperature distribution in the solid phase

consistent with the previous works [13-15]. If Θ and Y are defined as θ/θ_p and $-(y + L_p)/L_s$, respectively (where $\theta = T - T_\infty$ and $\theta_p = T_{p1} - T_\infty$), then the non-dimensional temperature distributions in the solid phase, for the various thicknesses of the sample are shown in fig. 4. It shows that for all thicknesses the curves tangent to the x axis at $Y = 0.95$ and the slope of the curves decreased with increasing the thicknesses of the sample.

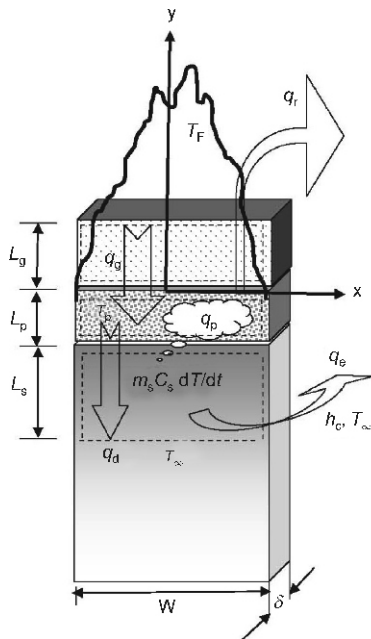


Figure 5. Control volume at the flame leading edge in the gas and solid phase

Theoretical consideration

Figure 5 depicts a downward flame spread over a sheet of arbitrary thickness in a flame fixed coordinate at the foot of flame. The horizontal and vertical axis are indicated by x and y , respectively. On a fixed coordinate, there is a flow of solid fuel in the negative direction of y at the velocity of V_f .

Scale up

To identify the relevant time and length scales, attention is focused on the leading edge of the flame where the fundamental mechanism of any flame spread occurs. Three control volumes, as shown in fig. 5 are investigated. The first region in the gas phase of size $W \times \delta \times L_g$, the second region in the thermal decomposition zone of size $W \times \delta \times L_p$, and finally, the third region in the solid phase of size $W \times \delta \times L_s$. W and δ are the sample width in the x direction and the thickness of the sample in the z direction, respectively. The length scales, L_g , L_p , and L_s in the y direction is unknown at this point.

In the control volume of gas phase, the volatiles and oxidizer react to raise the gas temperature from pyrolysis temperature T_p to a characteristic flame temperature T_f . In the control volume of thermal decomposition, gasification occurred in the constant pyrolysis temperature T_p . Finally, in the control volume of solid phase, the temperature change from its initial temperature T_∞ at $y = -(L_p + L_s)$ to the characteristic pyrolysis temperature T_p at the pyrolysis surface ($y = -L_p$).

Time scale

There are three characteristic times that their scales are as follows, in the gas phase:

$$t_g = \frac{L_g}{V_g} \quad (1)$$

where V_g is the velocity of volatiles from the solid surface into the gas phase due to advection. In the solid phase:

$$t_s = \frac{L_s}{V_f} \quad (2)$$

where V_f is the flame spread rate and L_s is estimated from the temperature distribution in the solid phase that is obtained by the experimental results in the previous section. The characteristic decomposition time is scaled as the time it takes for the pyrolysis reaction to produce the maximum possible amount of fuel vapor producing. Then in the thermal decomposition:

$$t_p = \frac{Q_s}{q_p} \quad (3)$$

where $Q_s = \rho_s L_s W \delta C_s (T_p - T_\infty)$ is the maximum heat stored in the solid, and $q_p = q_p W \delta$ is the heat consumed by the pyrolysis zone. To evaluate the effect of the pyrolysis kinetics, a zero order of Arrhenius law can be chosen.

The flame spread is obtained based on a few simplifying assumption as follows:

- steady-state process,
- the temperature is uniform throughout the thickness of the sample,
- all thermal properties of the fuel sample are constant,
- convection heat transfer coefficient is constant,
- movements of the volatiles within the liquid-like layer (pyrolysis region) are neglected,
- t_g is assumed to be large with respect to the characteristic chemical time justifying the assumption of infinitely fast chemistry,
- t_g is assumed to be small with respect to the radiative time scale justifying all neglected radiative effects, and
- t_p is assumed to be small with respect to t_s allowing the use of a constant pyrolysis temperature.

The spread mechanism, therefore, is completely heat transfer limited and the resulting regime is generally called thermal regime.

Length scale

In the gas phase, L_g can be obtained as the diffusion length in the y direction within the available characteristic time [16]. Since $T - t = \alpha_g^2 T / y^2$, then L_g can be obtained as:

$$L_g = \sqrt{\alpha_g t_g} \quad (4)$$

By substituting eq. (1) into eq. (4):

$$L_g = \frac{\alpha_g}{V_g} \quad (5)$$

In the solid phase and in a similar manner, L_s can be obtained as:

$$L_s = \sqrt{\alpha_s t_s} \quad (6)$$

By substituting eq. (2) into eq. (6):

$$L_s = \frac{\alpha_s}{V_f} \quad (7)$$

Note that the spread rates and the velocity of volatiles are still unknown in these expressions. The heat flux of radiation can be neglected for thin fuel [8, 17, 18], and then the spread rate from an energy balance for the pyrolysis control volume of fig. 5 is obtained as:

$$q_g = q_d = q_p \quad (8)$$

where q_g , q_d , and q_p , are the diffusion heat flux that is penetrated from gas phase to the gasification surface, the conduction heat flux diffused through the solid, and the heat flux that is consumed to degrade the solid phase, respectively. Each term and its order of magnitude in eq. (8) can be obtained as:

$$q_g = k_g \frac{\partial T_g}{\partial y} = k_g \frac{T_F - T_p}{L_g} \quad (9)$$

$$q_p = m_f h_v \quad \text{and} \quad m_f = \int_0^\infty \rho_s A_s \exp\left(-\frac{E_s}{RT_s}\right) dy \quad (10)$$

$$q_p = \rho_s A_s h_v L_p \exp\left(-\frac{E_s}{RT_p}\right) \quad (11)$$

$$q_d = k_s \frac{\partial T_s}{\partial y} = k_s \frac{T_p - T_\infty}{L_s} \quad (12)$$

The order of magnitude of energy flow (each term in eq. 8) can be calculated from the properties of tab. 1 and the results are listed in tab. 2. By comparing each term with the others, it is concluded that all of the terms have the same order.

Scaling rules [21] implies q_g and $q_d = q_p$ in eq. (8) to be the same order:

$$k_g \frac{T_F - T_p}{L_g} = k_s \frac{T_p - T_\infty}{L_s} = \rho_s A_s h_v L_p \exp\left(-\frac{E_s}{RT_p}\right) \quad (13)$$

Table 1. Property of PMMA and the characteristic lengths

Property	Value	Ref.	Property	Value	Ref.	Property	Value	Ref.
T_F [K]	1223	[3]	α_g [m^2s^{-1}]	$2.19 \cdot 10^{-5}$	[11]	R [$\text{Jmol}^{-1}\text{K}^{-1}$]	8.314	
T_p [K]	673	[3]	C_s [$\text{Jkg}^{-1}\text{K}^{-1}$]	1500	[3]	L_s [mm]	2.87	[*]
T_∞ [K]	300		C_{p_g} [$\text{Jkg}^{-1}\text{K}^{-1}$]	1005	[11]	L_g [mm]	0.36	[*]
k_s [$\text{Wm}^{-1}\text{K}^{-1}$]	0.19	[3]	h_v [Jkg^{-1}]	$1.356 \cdot 10^6$	[19]	L_p [mm]	0.20	[*]
k_g [$\text{Wm}^{-1}\text{K}^{-1}$]	0.02624	[11]	E_s [Jmol^{-1}]	$1.33 \cdot 10^5$	[20]	δ [mm]	1.75	
α_s [m^2s^{-1}]	$1.0644 \cdot 10^{-7}$	[3]	A_s [s^{-1}]	$2.92 \cdot 10^9$	[20]			

*Estimate from the present work

Due to mass conservation, reduced mass of the solid fuel equals the mass of volatiles; $m_s = m_v$ then:

$$V_f = \frac{\rho_g}{\rho_s} V_g \quad (14)$$

The flame spread rate can be estimated from the following relation, by substituting eqs. (5) and (6) into eq. (13):

$$V_f = F_T F_c \alpha_s \frac{1}{L_s} \frac{C_1}{\alpha_s C_s} \frac{1}{T_p - T_\infty} \quad (15)$$

where, F_T , F_c , and C_1 defines as:

$$F_T = \frac{T_p - T_\infty}{T_F - T_p}, \quad F_c = \frac{C_s}{C_{pg}}, \quad C_1 = A_s h_v L_p \exp \left(\frac{E_s}{RT_p} \right) \quad (16)$$

As discussed in previous section, L_s is proportional to δ for thin fuel and then we have:

$$V_f = F_T F_c \alpha_s \frac{1}{\delta} \frac{C_1}{\alpha_s C_s} \frac{1}{T_p - T_\infty} \quad (17)$$

Since all of the parameters except V_f and δ to be constant, then the relation between V_f and $1/\delta$, is linear. This result is identical to the previous experimental work of Mamourian *et al.* [13], theoretical study of Ayani *et al.* [14], Suzuki *et al.* [15], and Bhattacharjee *et al.* [3]. By substituting the properties of PMMA into eq. (17), it yields:

$$V_f = 0.1077 \frac{1}{\delta} \quad 0.0680 \quad (18)$$

In the other way the spread rate also can be obtained from an energy balance for the preheating control volume of fig. 5. Each terms and its order of magnitude can be obtained as:

$$q_{st} = \rho_s (\delta W) C_s V_f (T_s - T_\infty) \quad \rho_s (\delta W) C_s V_f (T_p - T_\infty) \quad (19)$$

$$q_c = h_c (2L_s W) (T_s - T_\infty) \quad h_c (2L_s W) (T_p - T_\infty) \quad (20)$$

$$q_d = k_s (\delta W) \frac{\partial T_s}{\partial y} \quad k_s (\delta W) \frac{T_p - T_\infty}{L_s} \quad (21)$$

where, q_{st} , q_c , q_d , and h_c are the stored energy in the solid phase, the convection heat transfer from the solid phase to the ambient, the conduction heat diffused through the solid phase, and the convection heat transfer coefficient, respectively. The non-dimensional forms of the above equations are listed in tab. (3).

With the similar manner in the previous paragraph, q_{st} , q_d , and q_c to be the same order. If $q_{st} = q_d$ then we have:

$$1 = \frac{\alpha_s}{V_f L_s} \quad (22)$$

Therefore, $V_f = \alpha_s / L_s$ and since $L_s = \delta$ then:

$$V_f = \frac{\alpha_s}{\delta} \quad (23)$$

Table 2. The maximum value and the order of magnitude of energy flow

Mode of energy	Formula	Value [kWm ⁻²]	Order of magnitude
q_g	$k_g \frac{T_F - T_p}{L_g}$	40.1	10 ²
q_d	$k_s \frac{T_p - T_\infty}{L_s}$	24.7	10 ²
q_p	$\rho_s A_s h_v L_p \exp \left(\frac{E_s}{RT_p} \right)$	40.1	10 ²

Table 3. Non-dimensional form of heat transfer mode in preheating zone

Energy store	Conduction	Convection
1	$\frac{\alpha_s}{V_f L_s}$	$\frac{2h_c \alpha_s L_s}{k_s V_f \delta}$

$$\text{If } q_{st} = q_c: \quad 1 = \frac{2h_c\alpha_s L_s}{V_f k_s \delta} \quad (24)$$

Therefore, $V_f = (2h_c\alpha_s/k_s)(L_s/\delta)$ and since $L_s \gg \delta$ then:

$$V_f = \frac{2h_c\alpha_s}{k_s} \quad (25)$$

Equation (23) shows that the relation between V_f and $1/\delta$, is linear and eq. (25) shows that V_f is a constant. By substituting h_c [21] and the properties of PMMA into the eqs. (23) and (25), these yields:

$$V_f = \frac{0.1064}{\delta} \quad (26)$$

$$V_f = 0.028 \quad (27)$$

For $O(\delta) \ll 1$ mm, $O(\delta) \approx 1$ mm, and $O(\delta) \gg 1$ mm the order of magnitude of eq. (26) is 10^{-1} , 10^{-2} , and 10^{-3} , respectively. While the order of magnitude of eq. (27) is 10^{-2} . By comparing eq. (26) with eq. (27), it is concluded that:

- for $O(\delta) \ll 1$ mm, eq. (27) can be neglected compare to eq. (26),
- for $O(\delta) \gg 1$ mm, eq. (26) can be neglected compare to eq. (27), and
- for $O(\delta) \approx 1$ mm, both equations must be considered.

Therefore, for all ranges of δ eqs. (26) and (27) yields:

$$V_f = 0.1064 \frac{1}{\delta} + 0.0280 \quad (28)$$

This result confirms previous discussion – eq. (18) – and the published experimental result by Ayani *et al.* [14]:

$$V_f = 0.1038 \frac{1}{\delta} + 0.0347 \quad (29)$$

Table 4. Slope of the linear variation and intercept of relation

	Slope of the linear variation [mm^2s^{-1}]	Intercept of relation [mms^{-1}]
eq. (18)	$1.077 \cdot 10^{-1}$	$6.80 \cdot 10^{-2}$
eq. (28)	$1.064 \cdot 10^{-1}$	$2.80 \cdot 10^{-2}$
eq. (29)	$1.038 \cdot 10^{-1}$	$3.47 \cdot 10^{-2}$

The slope of the linear variation and the intercept of relation presented in eqs. (18), (28), and (29) are listed in tab. 4.

By comparing each term with the others, it is concluded that all of the terms have the same order. But the discrepancies to bring out because of:

- the present work is based on the scale up method; therefore the constant values of the relation have the same order, and
- a few simplifying assumption is used in the analysis of the flame spread.

Conclusions

An experimental study of downward flame spread along vertical sheet of PMMA was conducted. An analytical model, based on the scale up, was also adopted to explain the flame spread mechanism. This approach was reasonably successful in predicting the flame spread rates. The following conclusions can be drawn from the results:

- the flame spread rate based on the thermal properties and the thickness of the sheet by scale up method is derived; it decreased inversely with increase the thicknesses of the sheet and reached to a constant value,

- since non-dimensional equations are used, it can be concluded that this method can be applied to other materials which have the physical behaviors like PMMA,
- the temperature profile shows, the temperature varies at the pyrolysis region (from 385 to 405 °C) and not to be constant, and
- the gradient temperature at solid phase decreases with increasing the thicknesses of the sample and the preheating length is proportional to the thickness of the sheet.

Nomenclature

A_s	– zero order pre-exponential factor, [s ⁻¹]
C_{p_g}	– specific heat of gas at constant pressure, [Jkg ⁻¹ K ⁻¹]
C_s	– specific heat of solid, [Jkg ⁻¹ K ⁻¹]
E	– activation energy, [Jmol ⁻¹]
h_c	– convection heat transfer coefficient, [Wm ⁻² K ⁻¹]
h_v	– enthalpy of volatiles, [Jkg ⁻¹]
k	– thermal conductivity, [Wm ⁻¹ K ⁻¹]
L	– length scale, [mm]
m	– rate of mass loss, [kgm ⁻² s ⁻¹]
q	– consumed heat, [W]
Q	– maximum heat, [J]
q	– heat flux, [Wm ⁻²]
R	– gas constant, [Jmol ⁻¹ K ⁻¹]
T	– temperature, [K]
t	– time scale, [s]
V_f	– flame spread rate, [mms ⁻¹]
W	– width of sample, [mm]

Greek letters

α	– thermal diffusivity, [m ² s ⁻¹]
δ	– thickness of sample, [mm]
ρ	– density, [kgm ⁻³]

Subscripts

d	– diffusion
F	– flame
f	– fuel
g	– gas phase
p	– pyrolysis
r	– radiation
s	– solid
st	– store
sur	– surround
v	– volatiles
∞	– ambient

References

- [1] Zeng, W. R., Li, S. F., Chow, W. K., Preliminary Studies on Burning Behavior of Poly Methyl Methacrylate (PMMA), *Fire Sciences*, 20 (2002), 4, pp. 297-317
- [2] Kashani, A., Esfahani, J. A., Interactive Effect of Oxygen Diffusion and Volatiles Advection on Transient Thermal Degradation of Poly Methyl Methacrylate (PMMA), *Heat and Mass Transfer*, 44 (2008), 6, pp. 641-650
- [3] Bhattacharjee, S., Wakai, K., Takahashi, S., Prediction of a Critical Fuel Thickness for Flame Extinction in a Quiescent Microgravity Environment, *Combustion and Flame*, 132 (2003), 3, pp. 523-532
- [4] Fangart, J., Wolanski, P., One Dimensional Analytical Model of Flame Spread over Solids, *Fire Sciences*, 9 (1991), 5, pp. 424-437
- [5] Ito, A., Kashiwagi, T., Temperature Measurements in PMMA during Downward Flame Spread in Air Using Holographic Interferometry, *Proceedings*, 21st Symposium (International) on Combustion, 1986, The Combustion Institute, Pittsburgh, Penn., USA, pp. 65-74
- [6] Esfahani, J. A., Kashani, A., One Dimensional Numerical Model for Degradation and Combustion of Polymethyl Methacrylate, *Heat and Mass Transfer*, 42 (2006), 6, pp. 569-576
- [7] Esfahani, J. A., Oxygen-Sensitive Thermal Degradation of PMMA: A Numerical Study, *Combust. Sci. and Tech.*, 174 (2002), 10, pp. 183-198
- [8] Fernandez-Pello, A. C., Williams, F. A., Laminar Flame Spread over PMMA Surfaces, *Proceedings*, 15th Symposium (International) on Combustion, 1975, The Combustion Institute, Pittsburgh, Penn., USA, pp. 217-231
- [9] Fernandez-Pello, A. C., Santoro, R. J., On the Dominate Mode of Heat Transfer in Downward Flame Spread, *Proceedings*, 17th Symposium (International) on Combustion, 1978, The Combustion Institute, Pittsburgh, Penn., USA, pp. 1201-1209
- [10] Hirano, T., Koshida, T., Akita, K., Flame Spread Mechanisms over PMMA Surfaces, *Bulletin of the Japanese Association of Fire Science and Engineering*, 27 (1977), 33

- [11] Krishnamurthy, L., Williams, F. A., On the Temperatures of Regressing PMMA Surfaces, *Combustion and Flame*, 20 (1973), 2, pp. 163-169
- [12] Ayani, M. B., Esfahani, J. A., Sousa, A. C. M., The Effect of Surface Regression on the Downward Flame Spread over a Solid Fuel in a Quiescent Ambient, *Thermal Science*, 11 (2007), 2, pp. 67-86
- [13] Mamourian, M., Esfahani, J. A., Ayani, M. B., The Effect of the Solid Fuel Dimensions on the Downward Flame Spread, *Proceeding*, 2th Combustion Conference of Iran (CCI-2), 2008, Mashhad, Iran, pp. 250-259
- [14] Ayani, M. B., Esfahani, J. A., Mehrabian, R., Downward Flame Spread over PMMA Sheets in Quiescent Air: Experimental and Theoretical Studies, *Fire Safety*, 41 (2006), 2, pp. 164-169
- [15] Susuki, M., Dobashi, R., Hirano, T., Behavior of Fires Spreading Downward over Thick Paper, *Proceedings*, 25th Symposium (International) on Combustion, 1994, The Combustion Institute, Pittsburgh, Penn., USA, pp. 1439-1446
- [16] Delichatsios, M. A., Heat Flux Distribution in Single Vertical Wall Fires, *Proceedings*, 26th Symposium (International) on Combustion, 1996, The Combustion Institute, Pittsburgh, Penn., USA, pp. 1281-1293
- [17] Williams, F. A., Mechanisms of Fire Spread, *Proceedings*, 16th Symposium (International) on Combustion, 1978, The Combustion Institute, Pittsburgh, Penn., USA, pp. 1281-1294
- [18] Fernandez-Pello, A. C., Hirano, T., Controlling Mechanisms of Flame Spread, *Combustion Science and Technology*, 32 (1983), 1, pp. 1-31
- [19] Krishnamurthy, L., Williams, F. A., Laminar Combustion of Polymethyl Methacrylate in O₂/N₂ Mixtures, *Proceedings*, 14th Symposium (International) on Combustion, 1973, The Combustion Institute, Pittsburgh, Penn., USA, pp. 1151-1164
- [20] Lengelle, G., Thermal Degradation Kinetics and Surface Pyrolysis of Vinyl Polymers, *AIAA*, 8 (1970), 11, pp. 1989-1996
- [21] Bejan, A., Convection Heat Transfer, John Wiley and Sons Inc., New York, USA, 2004

Author's affiliations:

M. Mamourian, M. B. Ayani
Mechanical Engineering Department,
Faculty of Engineering,
Ferdowsi University of Mashhad, Iran

J. A. Esfahani (corresponding author)
Mechanical Engineering Department,
Faculty of Engineering,
Ferdowsi University of Mashhad,
P. O. Box. 91775-1111, Mashhad, Iran
E-mail: jaesfahani@gmail.com